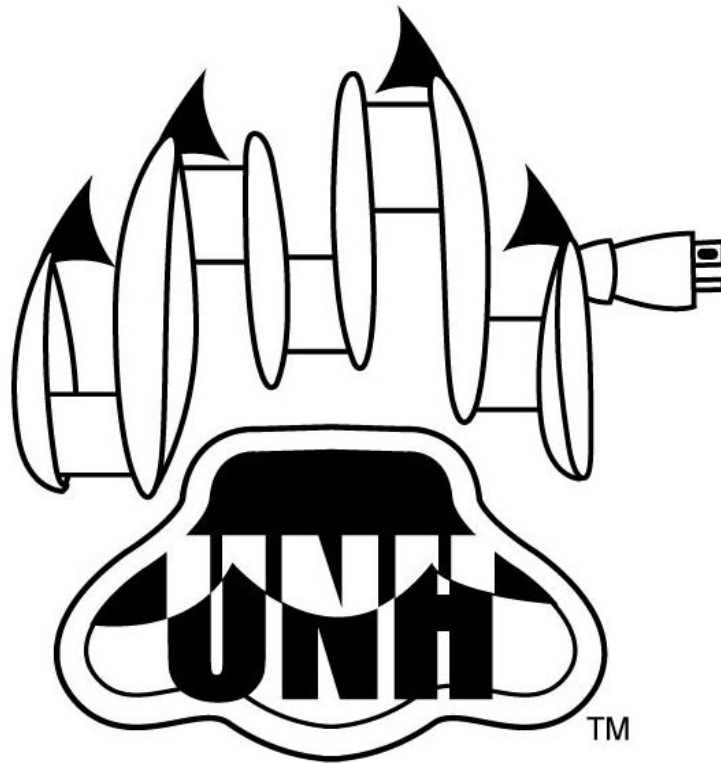


# Wave Energy

Mechanical Engineering Department  
University of New Hampshire

April 25, 2008



Michael Allard  
Colin Fischer  
Tania Grindrod  
Jessica Murray  
Kyle Russ

Advisor: Christopher White





## ACKNOWLEDGEMENTS

This project would not have been possible if it was not for the limitless help of many individuals, organizations, and corporations. The project was funded by the National Sea Grant College Program, NOAA, Department of Commerce, under grant #NA16RG1035 through the New Hampshire Sea Grant College Program, and through generous contributions from BAE Systems and Harold Davis. Many individuals provided much training and support throughout our design, construction, and testing phases of the project. Jud DeCew provided necessary training for the OPIE tracking system. Robert Champlin and Paul Lavoie provided much needed training on the machines in the machine shop as well as assisting in the making of very complex parts. Andy McLeod provided a valuable resource for using the wave tank as well as the data acquisition system. Thank you, Adam Perkins and Issam El Ayadi for supplying the necessary electrical components and electrical engineering advice. James Wright provided valuable background information for this project. Special thanks to the advisor of the project, Chris White. He provided guidance and advice and proved to be a valuable resource.



## **ABSTRACT**

To overcome the many problems related to anchoring and site placement, a buoy that does not have to be fixed by taut anchoring lines is the ideal choice. This allows greater flexibility in choosing a site of deployment. The final design takes advantage of relative displacement between two buoys. The two buoys include a modified torus shaped “follower” buoy as well as a long cylindrical shaped “spar” buoy. The spar and follower buoys have different inertias, thus creating relative displacement as they move with each other. Through prototype testing, dry testing of the final design, and final testing in the wave tank, it was possible to determine that the buoy operates at a maximum efficiency of 1.88%. It was found that the period and the amplitude have a direct correlation to the efficiency.



## TABLE OF CONTENTS

ABSTRACT.....	I
LIST OF FIGURES.....	III
LIST OF TABLES.....	V
1.0 INTRODUCTION .....	1
2.0 DESIGN .....	3
2.1.0 CHOOSING A BUOY SYSTEM.....	3
2.2.0 CHOOSING A POWER CONVERSION METHOD .....	4
3.0 OVERVIEW OF FINAL DESIGN.....	7
3.1.0 FOLLOWER BUOY DESIGN .....	8
3.2.0 SPAR BUOY DESIGN .....	9
3.3.0 POWER CONVERSION SYSTEM.....	10
4.0 TESTING .....	11
4.1.0 INITIAL PROTOTYPE TEST IN THE WAVE TANK .....	11
4.1.1 INITIAL PROTOTYPE WAVE RESPONSE MODEL .....	13
4.2.0 GENERATOR TEST .....	14
4.3.0 WAVE SIMULATOR TEST .....	17
4.4.0 SIMULATOR RESULTS.....	18
4.5.0 DEMONSTRATIVE CIRCUIT DESCRIPTION .....	20
4.6.0 BUOY WAVE TANK TEST .....	22
4.7.0 WAVE TANK TEST RESULTS.....	23
5.0 CONCLUSION .....	25
6.0 FUTURE DIRECTION OF THE PROJECT .....	27
REFERENCES .....	30
APPENDIX .....	A1



## LIST OF FIGURES

Figure 1: Methods of Power Conversion .....	4
Figure 2: Relative Displacement of Buoy .....	7
Figure 3: Final Buoy Design .....	8
Figure 4: Center of Mass .....	9
Figure 5: Power Conversion .....	10
Figure 6: OPIE Camera System.....	11
Figure 7: Buoy Prototype .....	12
Figure 8: Experimental Buoy System .....	13
Figure 9: Simulated Buoy System .....	14
Figure 10: Open-Circuit vs. RPM Plot.....	15
Figure 11: Power Curve for Generator .....	16
Figure 12: Efficiency Curve for Generator .....	16
Figure 13: Test Simulator .....	17
Figure 14: Power vs. RPM .....	18
Figure 15: Efficiency vs. RPM .....	19
Figure 16: LED Schematic.....	20
Figure 17: Full Wave Diode Bridge.....	20
Figure 18: Efficiency vs. Period .....	23
Figure 19: Dimensionless Parameter .....	24
Figure 20: Reservoir ( <a href="http://hydropower.id.doe.gov">http://hydropower.id.doe.gov</a> ).....	A2
Figure 21: Reservoir ( <a href="http://hydropower.id.doe.gov">http://hydropower.id.doe.gov</a> ).....	A2
Figure 22: Electro Magnetic ( <a href="http://hydropower.id.doe.gov">http://hydropower.id.doe.gov</a> ).....	A3



Figure 23: Oscillating ( <a href="http://www.fujitaresearch.com">http://www.fujitaresearch.com</a> ) .....	A3
Figure 24: Linear/Rotating Mechanical ( <a href="http://hydropower.id.doe.gov">http://hydropower.id.doe.gov</a> ) .....	A4
Figure 25: Static Equilibrium of Spar Buoy .....	A5
Figure 26: Calibration Dot .....	A5
Figure 27: Experimental Setup.....	A6
Figure 28: Windstream Power PMDC Generator Output Curves .....	A7
Figure 29: Time Constant of Rise with a Square Wave Input .....	A7
Figure 30: Time Constant of fall with a Square Input Wave .....	A8
Figure 31: Cam Design .....	A8
Figure 32: Crankshaft .....	A9
Figure 33: ProE Model of Simulator.....	A9



## LIST OF TABLES

Table 1: Buoy Design Decision Matrix .....	3
Table 2: Power Conversion Decision Matrix .....	5
Table 3: Wave Tank Tests .....	22
Table 4: Max Relative Displacement Peak to Peak .....	A11
Table 5: BOM for Buoy .....	A11
Table 6: BOM for Simulator .....	A13



## 1.0 INTRODUCTION

The world energy usage is continually increasing while the peak oil production is believed to be within the next 20 years. For this reason, it is necessary to seek out alternative sources of energy such as wind, wave, and tidal energy. There are many benefits to using wave energy. The power produced from waves is steady and more predictable than wind or solar energy. It is continuous and the waves can travel long distances without considerable energy loss. Waves contain about 1000 times more kinetic energy than the wind. Along with the benefit of having a renewable source of energy, wave energy provides environmental benefits. If designed correctly and placed in proper locations, ocean wildlife will remain undisturbed by the devices. Wave energy has a much more positive effect on the atmosphere than using fossil fuels.

Wave energy research is less developed compared to wind and solar. However, the cost per kilowatt is already in the same range as wind and less than solar devices. Current wind energy devices have a peak efficiency of 30% to 40% [4]. Presently the most efficient wave energy converter is approximately 15% and solar energy at 10% [5]. The theoretical maximum amount of energy that can be taken out of a wave is 50%, but practically the maximum is around 25% with an actual efficiency of 15% or less.

The objective of this project is to build a device that captures energy from a wave and converts mechanical wave energy into electrical energy. This is achieved by capturing the vertical motion of a wave and converting into electrical energy that can either be stored or immediately be used. The energy generated can be used to power offshore aquacultures, oil platforms, or





other offshore platforms. The time frame for this project is September 2007 to April 2008. With minimal time and resources, a scale model of the buoy was designed, built, and tested.

The outline of the report is as follows. In chapter two, a brief overview is given of the design process. An overview of the final design is provided in chapter three. Then the numerous tests and results are given in chapter four. These tests include generator tests, dry wave simulator tests, wave tank tests, and initial prototype tests. Lastly, a summary with conclusions is given in chapter five.



## 2.0 DESIGN

There are many ways to extract energy from the ocean. The key is to find the most efficient and cost effective way suitable for a particular site. Many different current designs try to maximize this efficiency. These designs were compared and important criteria were taken into account for the design of the buoy discussed in this report. For more information on the current designs please refer to the appendix.

### 2.1.0 Choosing a Buoy System

A decision matrix was constructed to help the Wave Energy team decide which type of buoy system was best for the team to design, build, and test in one school year. Time, money and resources had to be accounted for in the decision matrix. Table 1 shows the decision matrix used to score the various designs considered. The categories on the left are weighted by importance in the decision process. Size was important since the wave tank is only suitable for objects under two feet wide. The design must be simple yet, durable enough to withstand the harsh ocean life; constantly changing waves, high winds and salt water. The buoy should have low environmental impact in order to not disturb the wildlife in the area. Aesthetics were judged, but only weighted as a one.

**Table 1: Buoy Design Decision Matrix**

		Reservoir		Electro/Mag		Oscillating		Linear Mechanical		Rotating Mechanical	
Categories	Weight	Score	Total	Score	Total	Score	Total	Score	Total	Score	Total
Size	3	0.1	0.3	0.3	0.9	0.3	0.9	0.3	0.9	0.3	0.9
Ability to Test	5	0.1	0.5	0.3	1.5	0.3	1.5	0.3	1.5	0.3	1.5
Complexity (ability to build)	5	0.3	1.5	0.1	0.5	0.3	1.5	0.1	0.5	0.3	1.5
Durability	5	0.3	1.5	0.3	1.5	0.2	1	0.3	1.5	0.2	1
Environmental Impact	3	0.1	0.3	0.3	0.9	0.2	0.6	0.3	0.9	0.3	0.9
Aesthetics	1	0.1	0.1	0.2	0.2	0.2	0.2	0.2	0.2	0.2	0.2
Total Score			4.2		5.5		5.7		5.5		6

The rotating mechanical design scored best in the decision matrix. Importantly, it scored well in all of the categories, and the design is simple enough that it can be built in the short time frame available. Drawbacks of the other systems considered are summarized as follows: The reservoir system is too large to fit in the UNH wave tank. In addition, ocean debris entering the reservoir is problematic. The electromagnetic system is too complex for a group of mechanical engineers. The oscillating buoy scored poorly because it has a complex mooring system and power conversion is complicated; the linear mechanical design was found to be too expensive.

### ***2.2.0 Choosing a Power Conversion Method***

There are multiple methods used to convert the mechanical energy of the buoy to electrical energy in the rotating mechanical design. Table 2 shows another decision matrix that was used to decide the power conversion. Figure 1 shows examples of the different types of power conversion devices considered in Table 2. The important parts of power conversion include size, ability to test, complexity and durability: it cannot be too large because it has to fit inside the buoy; it must be easy to test; it cannot be too complex to build; it also must be durable.

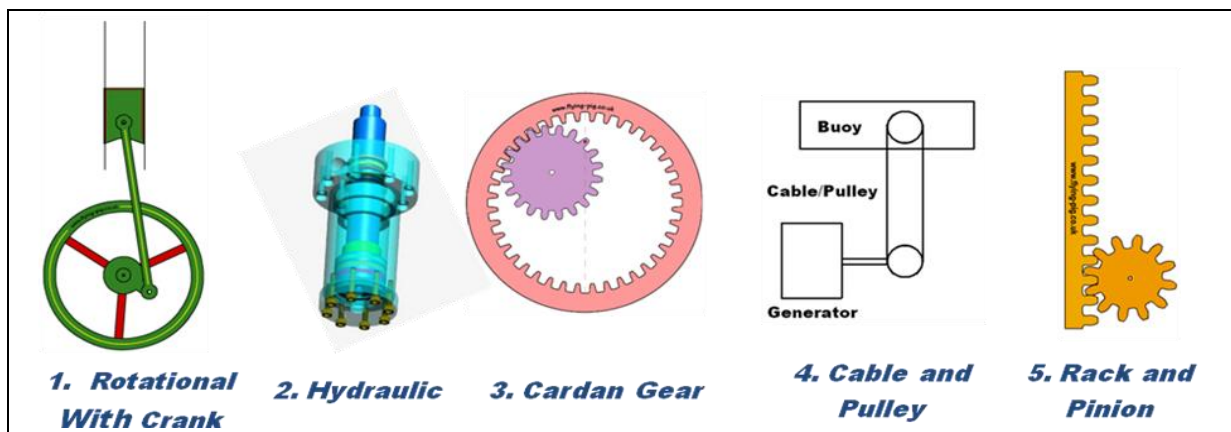


Figure 1: Methods of Power Conversion

**Table 2: Power Conversion Decision Matrix**

Power Conversion		Rotational w/ Crank		Rack and Pinion		Cardan Gear		Cable and Pulley		Hydraulic	
Categories	Weight	Score	Total	Score	Total	Score	Total	Score	Total	Score	Total
Size	3	0.2	0.6	0.3	0.9	0.2	0.6	0.3	0.9	0.4	1.2
Ability to Test	5	0.2	1	0.3	1.5	0.3	1.5	0.3	1.5	0.2	1
Complexity (ability to build)	5	0.2	1	0.3	1.5	0.1	0.5	0.2	1	0.1	0.5
Durability	4	0.3	1.2	0.3	1.2	0.3	1.2	0.1	0.4	0.3	1.2
Total Score			3.8		5.1		3.8		3.8		3.9

The first conversion system is similar to a piston in a car; the buoy would be the piston and move up and down while the crank spins a generator. This device is good because both the up and down motion of the buoy would spin the generator in the same direction. The disadvantage is if the waves are not big enough a full rotation will not occur and there would be no energy generated. The second conversion type uses hydraulics. This could be very efficient and effective, but is very complex and difficult to scale. The third idea with the Cardan gear has the same problem as the piston; the waves always have to be big enough in order to get electricity out. The fourth idea of a cable and pulley is good because it does not rely on an exact wave height to extract power. The problem with this design is that it is difficult to gear up: the waves are not going to be high enough to get a lot of rotations on the motor therefore there must be a gear train to get more rotations on the motor. The final rack and pinion design was found to be the best option for power conversion. The idea is that the pinion would stay fixed while the rack goes up and down with the waves. A long enough rack will be able to account for various wave heights. Having a round pinion gear allows for a gear train to optimize motor rotation. The downfall of this conversion system is that the pinion stops and changes direction at the top and bottom of each wave. There are two ways to overcome this: the first is to use a clutch where the gear will not spin the motor on the down stroke. (This method is not



very efficient because it only uses half of the energy that is available.) The second is to use a two-way generator that generates electricity independent of the direction of rotation.



### 3.0 OVERVIEW OF FINAL DESIGN

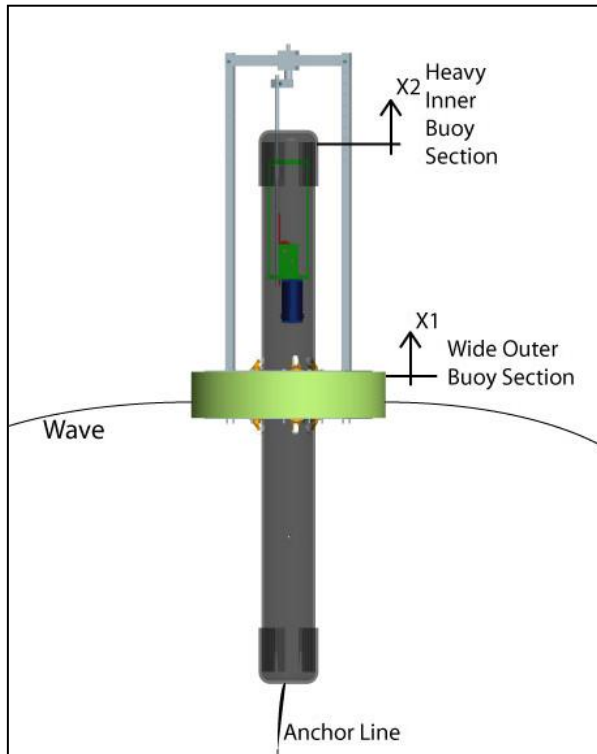


**Figure 2: Relative Displacement of Buoy**

The final design takes advantage of relative displacement created by two buoys of different inertias moving with each other. To overcome the many problems related to anchoring and site placement a buoy that does not have to be fixed by taut anchoring lines is an attractive choice. This allows greater flexibility in choosing a site. The overall buoy concept consists of two sub-buoys, a modified torus shaped “follower” buoy as well as a long cylindrical shaped “spar” buoy. The spar moves within the center hole of the follower, as can be seen in Figure 2. The

relative displacement,  $\Delta x$ , can be found using the following relation:

$$\Delta x = |x_2 - x_1|$$

Where  $x_1$  is the displacement of the follower buoy and  $x_2$  is the displacement of the spar buoy. The two sub-buoys will also act out of phase with each other helping to create a larger relative displacement,  $\Delta x$ .



### 3.1.0 Follower Buoy Design

The follower is a solid foam torus. Mounted to this is a rigid, aluminum frame that transfers the motion of  $x_1$  to the swivel. In turn the swivel transfers the motion of the follower to a shaft on to which a rack is mounted. The swivel, as the name suggests, allows the follower buoy to rotate if necessary, without effecting the motion of the spar buoy. Note that this assumes that the effect of friction between the spar buoy and the follower mounted casters is negligible. Small casters can be

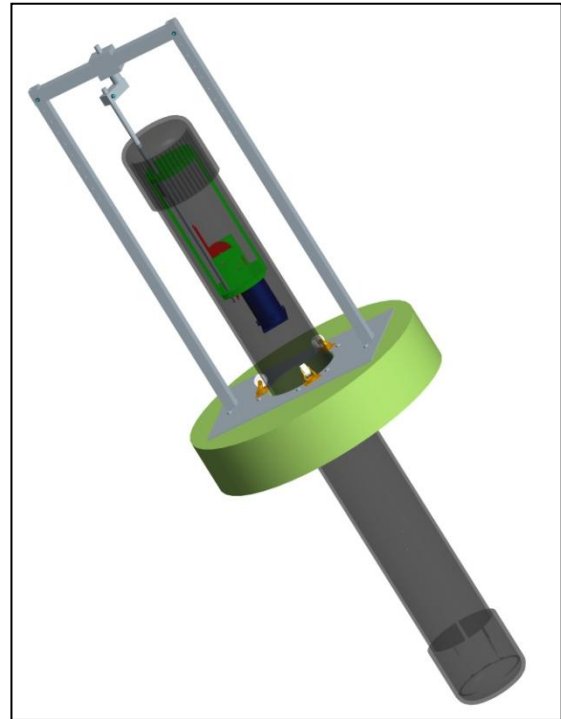


Figure 3: Final Buoy Design

seen in Figure 3 mounted to the top and bottom of the follower buoy. The casters act to stabilize the motion between the spar and the follower buoys. This ensures that the follower and the spar will displace in a uniform direction, meaning that the spar buoy will not tilt within the follower buoy. To give an idea of the size of the final prototype design, the follower is 25in in diameter and the central hole is 7.125in in diameter. The rigid aluminum frame is adjustable, allowing the swivel position to move up and down. This allows for the spar and follower to statically float neutrally compared to each other even if the weight of either buoy is affected. The follower buoy has a total weight of 20.5 lbs and has static buoyancy equilibrium of 1.13in submerged. The reserve buoyancy volume is 1963 in<sup>3</sup>. This will provide a reserve buoyant force of 70.43 lbf.



### 3.2.0 Spar Buoy Design

The cylindrical spar buoy is specifically shaped in order to let the waves pass around the buoy with less of an effect on the amplitude of its displacement. The buoy is composed of schedule 40 PVC with two end caps. The bottom end cap provides an anchor point in order to keep the buoy from floating away. The spar buoy measures 63.5in in total length at a diameter of 6.625in.

This provides plenty of internal space for the power conversion and electricity to take place. This prototype does not contain a battery for storage; the electricity produced is transported directly out of the buoy to a demonstrative light source.

When deployed in the ocean it is possible that the energy will be stored on board the buoy. In order to simulate this energy storage method weights have been placed in the bottom of the spar buoy. Locating the energy storage in the bottom, or submerged section of the spar buoy serves to sink

the heat away from the batteries and into the cool ocean water. It also serves the purpose of lowering the center of mass of the buoy (seen in Figure 4), this allows for more stability and less threat of tipping due to a storm or rough wave.

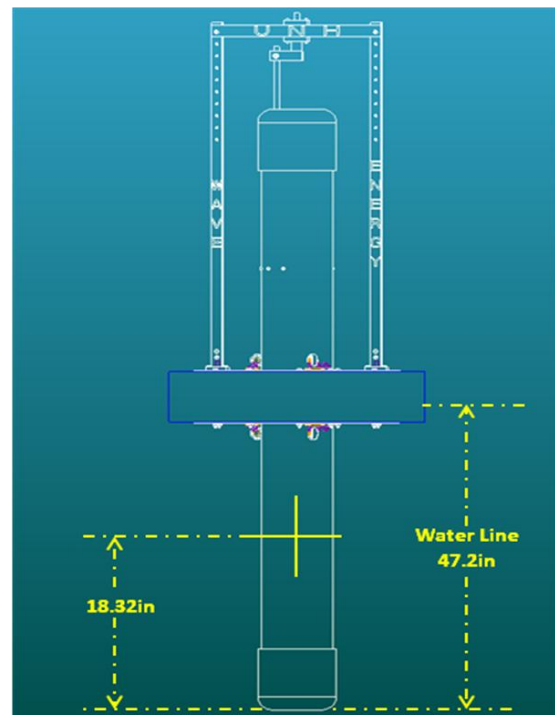


Figure 4: Center of Mass





### 3.3.0 Power Conversion System

The spar buoy holds the power conversion system (seen in Figure 5) which consists of: a gear train, a rack and pinion and a permanent magnet DC (PMDC) generator. The rack is attached to

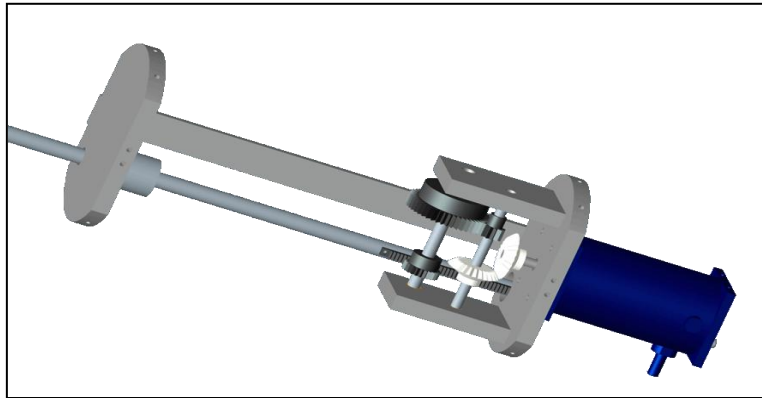


Figure 5: Power Conversion

a shaft that moves linearly with the up and down motion of the wave and displaces an amount  $\Delta x$ . This linear motion is converted to rotary motion through the use of a pinion. The gear train transfers this energy from the pinion to the

PMDC generator. The gear train serves to increase the velocity of the buoy motion at the generator by about four times. This allows the generator to produce power at a more usable range. The generator will produce power at any speed under 5000 RPM. The operating range of the PMDC generator in the buoy seen in testing was between 0 and 410 RPM.



## 4.0 TESTING

There were multiple tests done in the buoy design process. The first test was in the fall semester. The purpose of this test was to determine if relative displacement was feasible for the Prototype Test in the Wave Tank. The next test was the testing of the PMDC generator to see if it could perform at the low angular velocities it would see on the buoy. The third test was of the final prototype in the wave simulator. Testing of the buoy before it is put into the water is crucial to make sure everything works before the risk of water damage comes into play. The final test was performed in the wave tank using the final prototype.

### 4.1.0 Initial Prototype Test in the Wave Tank



**Figure 6: OPIE Camera System**

The wave tank located in Chase Hall played a key role in the design and testing of the wave energy device. In the initial design phase, the wave tank was used to find if relative motion existed between the spar and follower buoys. The relative motion between the buoys had to be quantified; the Optical Positioning Instrumentation and Evaluation (OPIE) camera system was used to do this, seen in Figure 6. The software for OPIE tracks small black dots located

on the spar and follower buoys and converts the motion using a Matlab code.



Once the waves of the tank are set in motion, one black dot on the spar and follower are selected, and they are tracked for roughly ten seconds. The software then reveals a plot of the motion of both black dots. The amplitudes and difference in phase revealed the amount of relative motion that existed between the spar and follower buoy.

The OPIE system was initially used on a prototype buoy that was built to investigate the relative motion between the spar and follower

buoys. This prototype is shown in Figure 7. The black squares seen on the spar and follower are used by OPIE to track the buoy motion. Using the OPIE system it was found that the prototype provided relative motion between the spar and follower. The results obtained from OPIE were plotted and compared with a theoretical model constructed in



**Figure 7: Buoy Prototype**

Matlab SIMULINK to predict the amount of relative motion. This model was beneficial to allow for the prediction of the response of the buoy system under various wave conditions. It also provided a means of predicting the response of the buoy system in the ocean with real waves.



#### 4.1.1 Initial Prototype Wave Response Model

As this project proceeds and is scaled up in size it is important to be able to predict the behavior of the larger model in the ocean. To do this a model was developed using Matlab and Simulink. For more information on how the model works and a schematic of the Simulink diagram please refer to the Appendix. Figure 8 and Figure 9 show the comparison of the computer model to experimental results obtained using the initial prototype. The computer model matches very well to the experimental model confirming its predictive functionality.

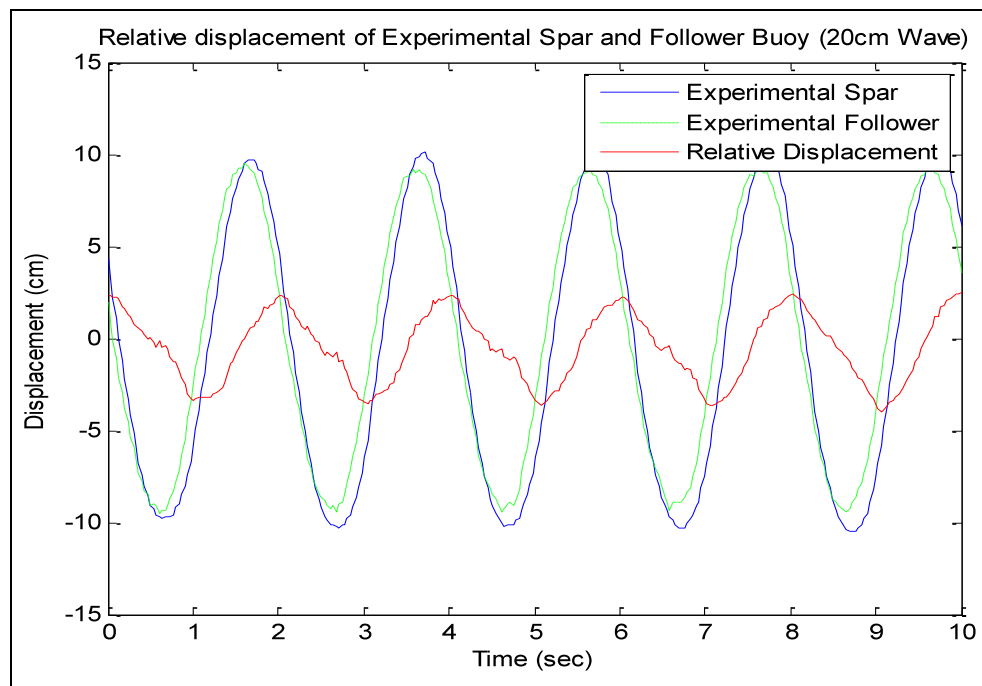


Figure 8: Experimental Buoy System

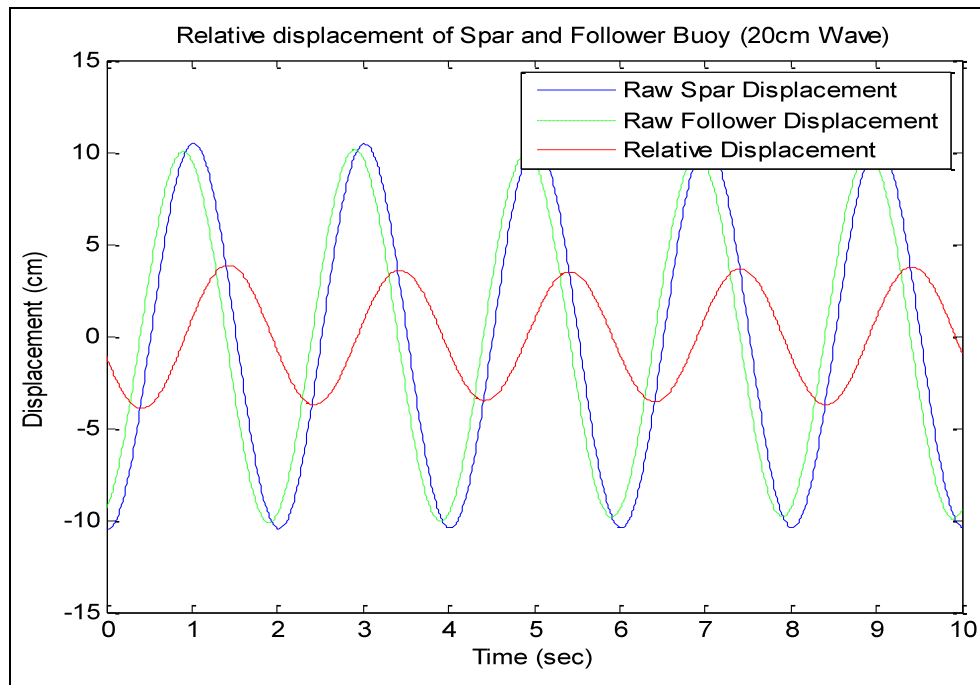


Figure 9: Simulated Buoy System

#### 4.2.0 Generator Test

A generator is used to convert the mechanical energy of the waves into electrical energy. Since the wave amplitude is expected to be small, the generator will have low angular velocities. Thus, a generator capable of spinning at low angular velocities is required. The generator will rotate both clockwise and counterclockwise with the rise and fall of the pinion on the rack, so using a generator that can capture energy in both directions is preferable. A Windstream Power, permanent magnet direct current (PMDC) generator, met all the design criteria stated above.



A few parameters of the generator needed to be tested.

To test the generator given a known input, it was driven by another motor. The two motors were connected using a helical beam coupling, which allowed flexing due to misalignment. The test results

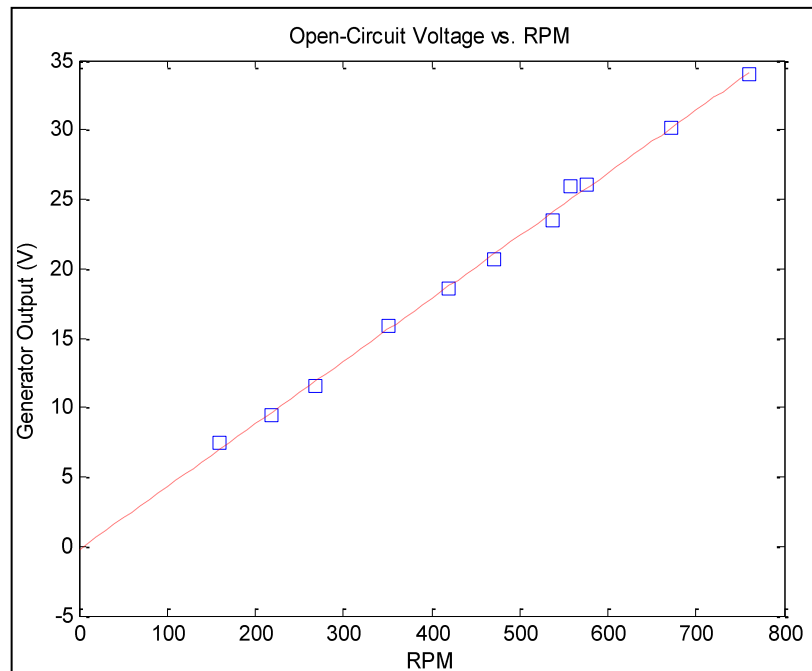
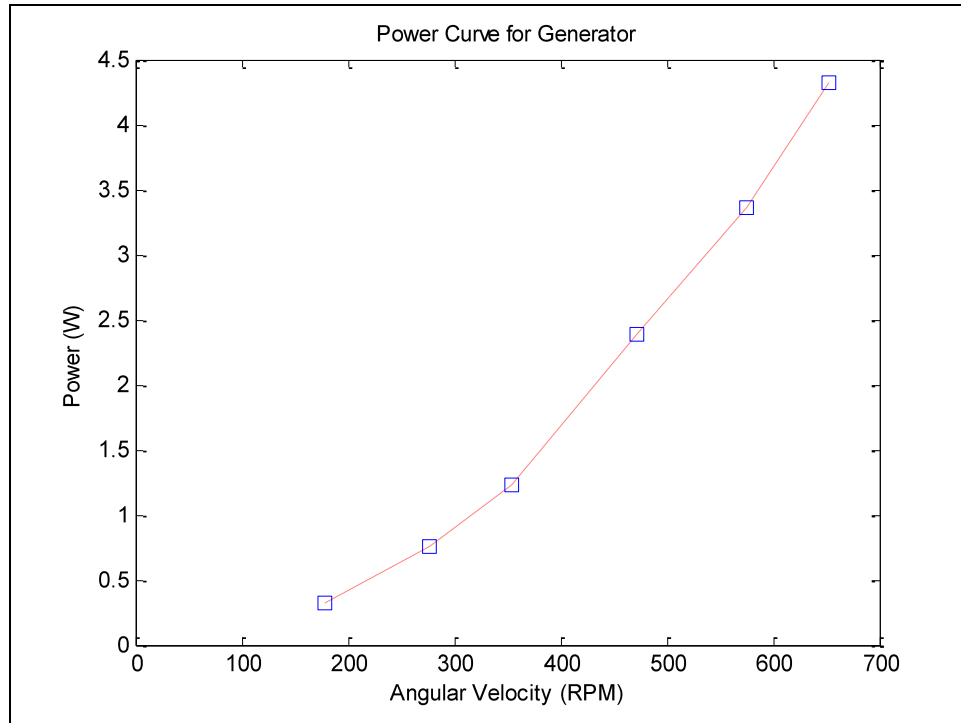


Figure 10: Open-Circuit vs. RPM Plot

yielded time constants of

$2.9 \times 10^{-2}$  s for the rise and  $5.4 \times 10^{-2}$  s for the fall. This confirms that the generator reaches steady-state value quickly and there is not much lag.

To confirm the open-circuit voltage ( $V_{oc}$ ) versus angular velocity plot provided by Windstream Power, the  $V_{oc}$  of the generator was measured with an oscilloscope while varying the angular velocity of the drive motor, see Figure 10. This compares very well with the plot supplied by Windstream Power that can be seen in Appendix A. In addition to verifying the  $V_{oc}$ , the generator was also back driven to obtain a power curve as well as an efficiency curve, see Figure 11 and Figure 12.



**Figure 11: Power Curve for Generator**

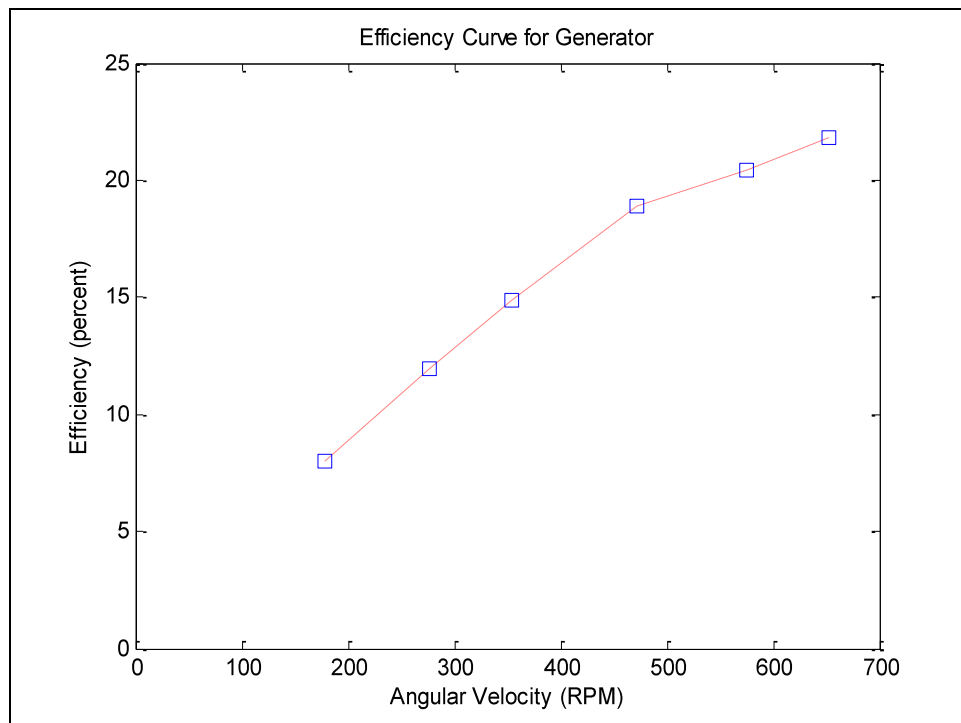


**Figure 12: Efficiency Curve for Generator**



### 4.3.0 Wave Simulator Test



When testing in water, it is possible that the item being tested is not water tight due to faulty seals, housings, etc. A source of water leakage could damage the item being tested. In the case of this wave energy device, having a watertight prototype is extremely crucial because of the intricate electronic components housed within. If the electronic components failed due to water damage in the early stages of wave tank testing, there would be limited to no results. Therefore, it would not be known how much energy the buoy could generate. For this reason, a wave simulator was constructed to obtain results to reveal an ideal energy conversion of the wave energy device out of the water. The simulator was also beneficial to ensure that all of the components of the buoy operate well together and function properly.

A test fixture was built to test the wave energy device outside of the wave tank, see Figure 13. The test fixture simulated wave motion by

propelling the spar buoy upward while holding the follower buoy stationary.

The amplitude of typical relative displacement, 10cm, was chosen for the test fixture. This was determined because of the relative motion between the spar and follower buoys seen in testing of the original prototype. The original prototype had a relative displacement of roughly 10 cm when the wave amplitude was actually 20 cm. The simulator drive motor was operated at





variable voltages from roughly five volts up to the maximum rated voltage of 24V. This was performed in order to find the optimal frequency, i.e. wave period, for energy generation. The drive motor was capable of supplying the system 180 in-lbf of torque.

#### **4.4.0 Simulator Results**

The wave energy device does not output continuous power. This is because the shaft of the generator spins in one direction as the follower moves up the spar, and in the opposite direction as the follower moves down the spar. Due to this type of motion, energy generates sinusoidal in nature. Figure 14 below shows the peak power generated with respect to angular velocity. It can be seen that the peak output power of the wave energy device was at roughly 31 RPMs.

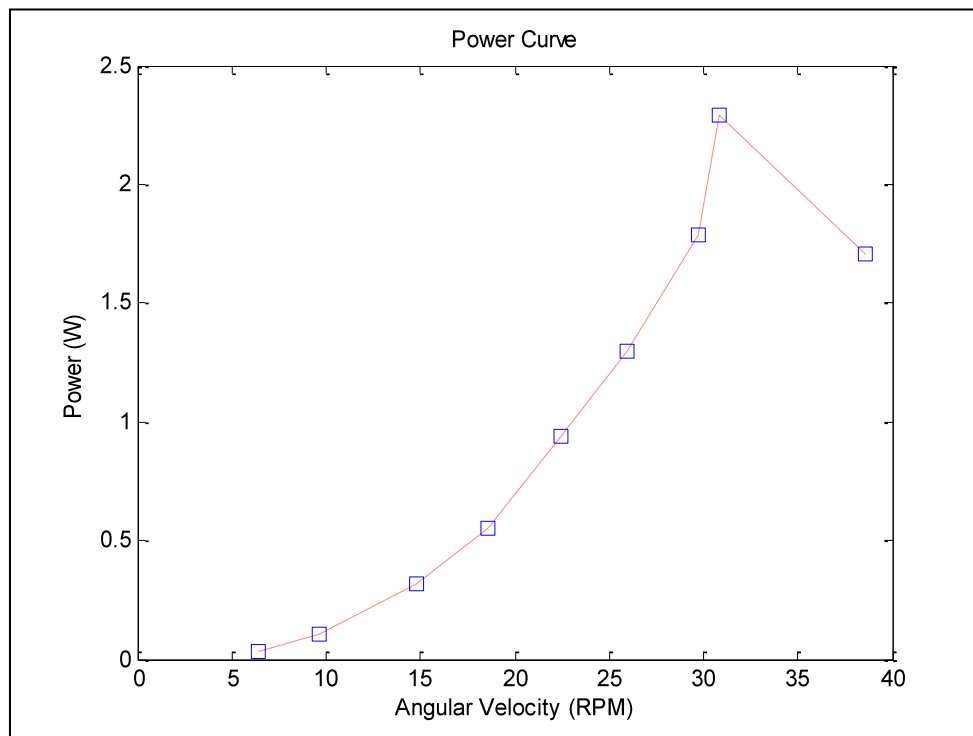


**Figure 14: Power vs. RPM**



In order to vary the rotational speed of the wave energy device, the supply voltage of the simulator was adjusted. The angular velocity was found by reading the time it took for the spar to move from the lowest to highest position on the simulator. This motion corresponded to  $180^\circ$  of crankshaft rotation, or one half of a revolution. A full revolution was not used to find the RPMs because the weight of the spar increased the speed of the motor as the spar moved downward. It should be noted that the time readings were accurate to the thousandths place due to the accuracy of the oscilloscope that was used.

From the power curve shown above, efficiency vs. RPM curve was generated, as seen in Figure 15. Once again, it can be seen that the wave energy device is most efficient at roughly 31 RPMs.

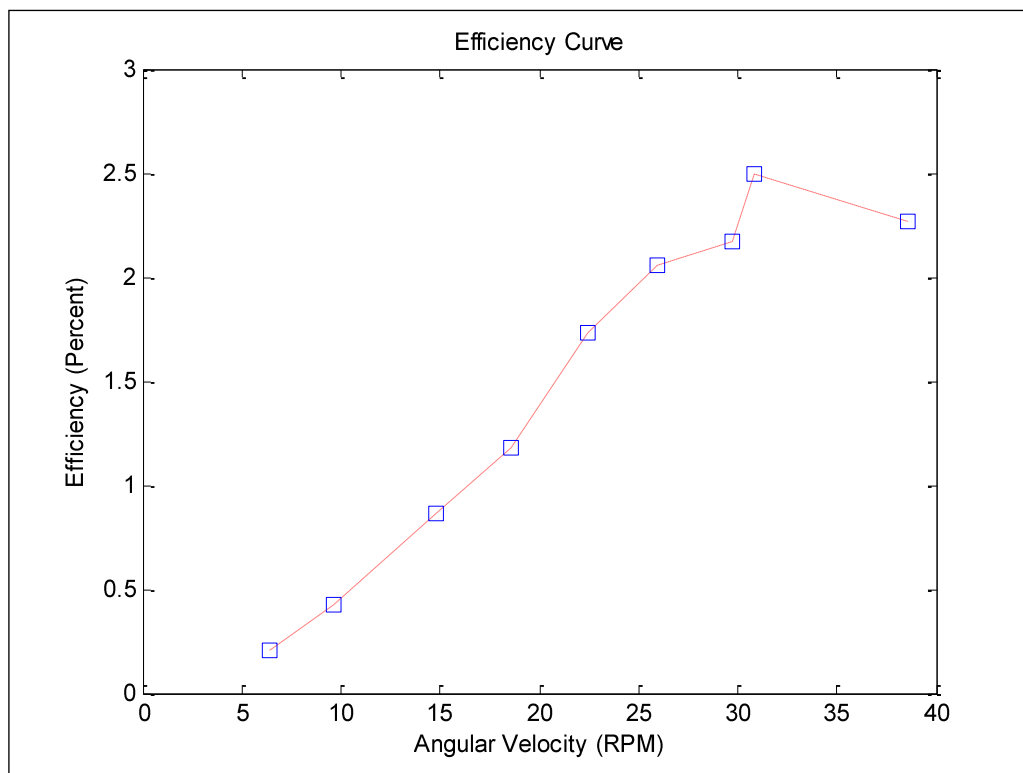


**Figure 15: Efficiency vs. RPM**

#### 4.5.0 Demonstrative Circuit Description

To provide proof that our buoy system can capture the energy from a wave and convert it into electrical energy the generator output was attached to a light emitting diode (LED) circuit that spells out UNH, see Figure 16.

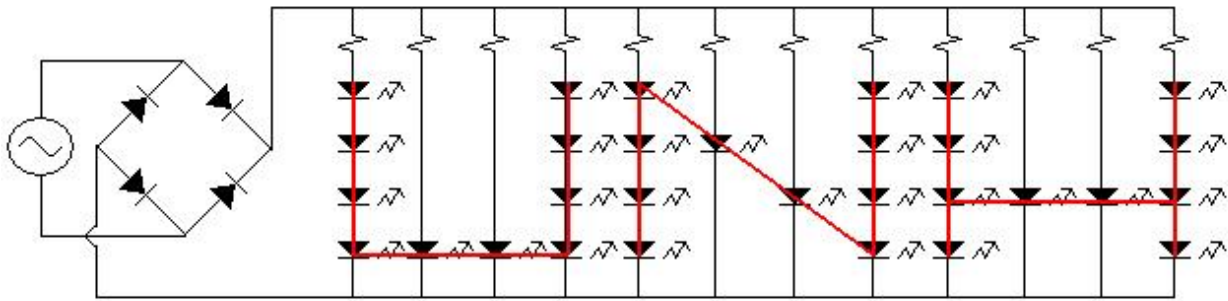


Figure 16: LED Schematic

The circuitry consists of a full wave diode bridge, thirty red LEDs, and various resistors. Since the polarity of the output from the generator constantly reverses, a full wave diode bridge is used to keep a constant polarity to the LEDs, see Figure 17 below.

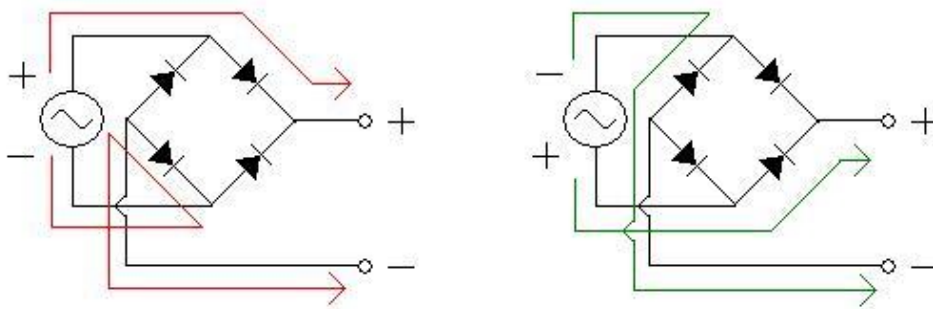


Figure 17: Full Wave Diode Bridge

If the bridge is not used, the LEDs would only light up for either clockwise or counterclockwise shaft rotation. Note that there is approximately a 1.2V voltage drop across the bridge (0.6V per



diode and it passes through only two diodes at one time). In addition, some of the LEDs are in series and some are in parallel. This is why various resistors are needed. Since each LED has a voltage drop of approximately 1.8V, the total voltage drop required to spell out the letters varies depending on the string and the number of LEDs to make the letter in that particular string. For example, four LEDs are needed to make the left portion of the letter U, while only one is needed for the next column, refer to Figure 16. Thus to have the same current flowing through each column, since current takes the path of least resistance, the resistors are used to equate the resistances of each parallel line. The LEDs used in the circuit are capable of handling between 0mA to 20mA, therefore by knowing this information, the highest possible voltage seen by the circuit, and the total voltage drop, the amount of added resistance required can be calculated as follows. First determine the maximum voltage expected out of the generator. Subtract the voltage drop of the bridge and the voltage drop per LED (voltage adds in series). Divide this result by 15mA to provide a safety factor since they can only handle up to 20mA.

When the generator changes rotational direction, flashing occurs because for a moment no output power is being produced. A capacitor can be inserted into the circuit and charge up with the excess power not needed by the LEDs. When the rotation of the generator is changing direction, the capacitor would discharge keeping the LEDs lit. A blocking diode would also be needed to prevent current from flow back into the generator. Another future goal is to light a series of light bulbs.



#### 4.6.0 Buoy Wave Tank Test

The wave tank was utilized in the second semester to test the fully functioning final prototype. In order to measure the power output from the generator in the wave tank, a variable power resistor was used as the load. The load resistance was adjusted until a value was found that allowed for reasonable relative motion between the spar and follower buoys, and therefore shaft rotation of the generator. The voltage drop across the load resistance was recorded in real time on the oscilloscope as the buoy system responded to the waves. This voltage drop yielded the current leaving the generator using Ohm's Law,  $V=IR$ .

The buoy was tested in the wave tank under various conditions. Table 3 summarizes the fifteen combinations of wave amplitudes and periods tested.

**Table 3: Wave Tank Tests**

<b>Amplitude 1</b>		<b>Amplitude 2</b>		<b>Amplitude 3</b>	
<i>Amplitude (cm)</i>	<i>Period (s)</i>	<i>Amplitude (cm)</i>	<i>Period (s)</i>	<i>Amplitude (cm)</i>	<i>Period (s)</i>
10	1.0	15	1.0	20	N/A
10	1.1	15	1.1	20	1.2
10	1.2	15	1.2	20	1.3
10	1.3	15	1.3	20	1.4
10	N/A	15	1.4	20	1.5
10	N/A	15	1.5	20	1.6

The buoy was held in position by two strings until the waves were set in motion. At this point, the strings were released and the buoy had no external forces acting on it. The data was recorded while the buoy was free to float on its own. This method was used to simulate how the buoy will perform in actual deployment, where it will not be rigidly anchored.

The waves within the tank were measured simultaneously for their amplitude and period using a wave staff. This device is simply placed in the water at the water line. The device then



records how high the waves travel on the staff, as well as the period between waves. The information gets recorded on a computer, which is also used to control the waves.

Aside from testing the buoy system for its efficiency, an LED circuit was used as the load on the generator for a visual representation of the energy generated by the device. The LED's lit up as the buoy moved up and down with the waves providing power to the circuit. This test was performed strictly for demonstrative purposes. No data was obtained from this test.

#### 4.7.0 Wave Tank Test Results

For each wave period and amplitude tested in the wave tank, the efficiency of the wave energy device was calculated. Figure 18 shows the plot of the efficiency versus the wave period for each of the three amplitudes tested.

The efficiency was calculated from an average power value found by integrating under the instantaneous power curve as the follower buoy traveled one complete cycle of the wave. It can be seen in the plot that the

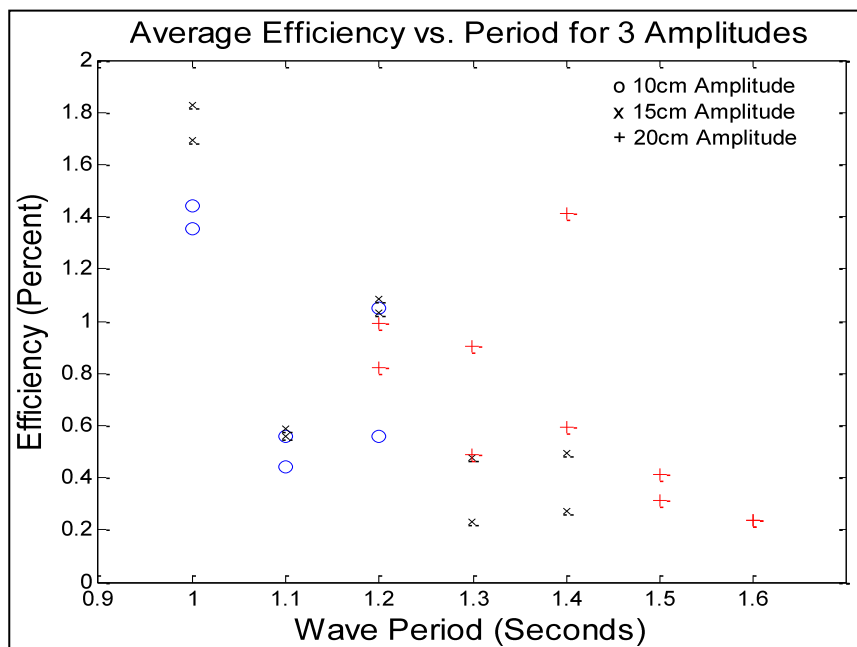


Figure 18: Efficiency vs. Period



most efficient wave period was one second.

This result is conceptually valid because the relative velocity of the spar to the follower is greater with a shorter period. It can also be seen on the plot that the larger wave periods did not produce any energy for the lower wave

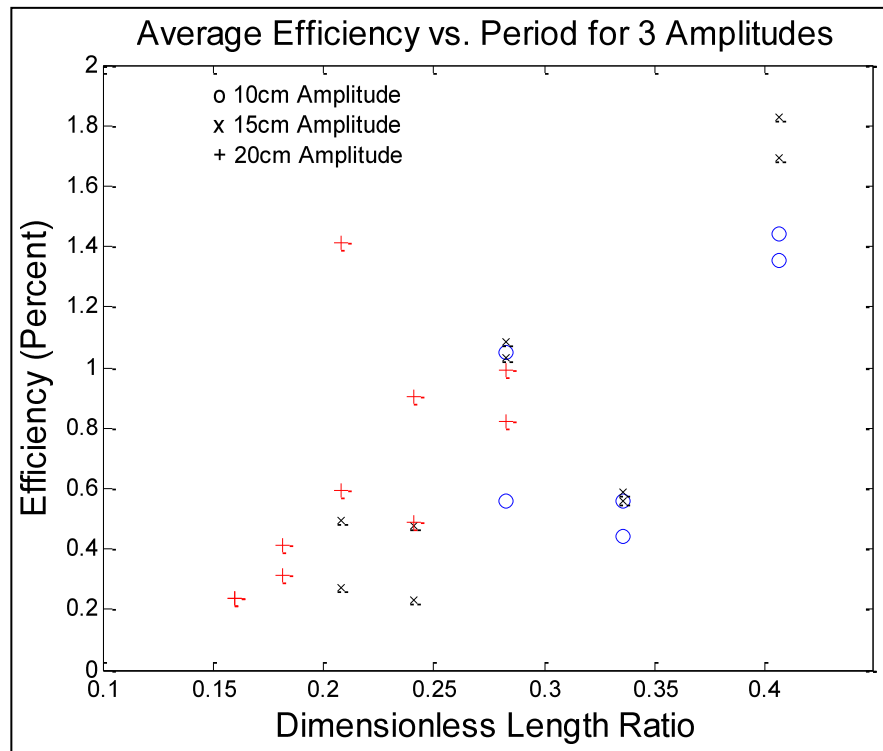


Figure 19: Dimensionless Parameter

amplitudes. This suggests that an optimum period can be found based on buoy size.

To investigate period vs. buoy size an efficiency plot was also generated with respect to a dimensionless length parameter. The dimensionless length parameter is a ratio of the diameter of the follower to the wave lengths in the tank. Figure 19 shows the efficiency with respect to the dimensionless ratio.

It can be seen from the plot that the efficiency of the device increases as the dimensionless ratio increases. However, this trend may end after the dimensionless ratio reaches a certain value.



## 5.0 CONCLUSION

The project was successful in that the team designed, built, and tested a buoy that converts wave energy to electrical energy in one school year. There were multiple types of energy converters researched, and they were narrowed down using a decision matrix. The final design of the buoy used a mechanical conversion system consisting of a rack and pinion that utilized the relative displacement between the two sub-buoys. The two sub-buoys of the final design consists of a spar and follower where the spar does not move much with respect to the waves while the follower moves up and down with the motion of the waves. Attached to the follower is a rack that connects to a gear box within the spar. The gear box has a four to one gear ratio to increase the number of revolutions of the PMDC generator as the spar and follower move relative to one another. The total cost of the buoy was \$1100 and the simulator cost \$500. There were also some small costs in preliminary testing.

The buoy was first tested using a wave simulator. The simulator moves the spar the amount of relative displacement seen from the waves of the wave tank. The maximum power out of the generator when subjected to a 10cm amplitude wave simulation was found at 31RPM from the drive motor. The maximum power was approximately 2.4W with a maximum efficiency of 2.5%. When the buoy was tested in the wave tank, it was found that the most efficient wave period was one second with a 15cm wave amplitude. The maximum efficiency in the wave tank was 1.88%. The maximum efficiency from the 10cm wave height was 1.45%. This is accurate when compared to the simulator efficiency of 2.5% at 10cm amplitude. It was expected that the efficiency would decrease when put into the water. This is because the buoy has the drag of the





water against it and also has more than just vertical forces acting on it. This project has successfully laid the groundwork for a wave energy program at the University of New Hampshire.



## 6.0 FUTURE DIRECTION OF THE PROJECT

With the inductance of wave energy to UNH's Ocean Engineering Department, it is the hope that the project continues to grow and foster revolutionary ideas and methods for both extracting energy and quantifying efficiencies. Although the project is still in its early stages, it has been successful in providing a platform on which to build an extensive wave energy program. The team this year was composed of five mechanical engineers. As growth develops it will be important to extend this project to include an interdisciplinary team, with emphasis on mechanical, ocean, and electrical engineers although marine biologists will likely be important for environmental impact studies. There are four main areas of expansion and development needed. These include, involved site analysis, scaling prototype up to full size, anchoring system design, and finally maximizing efficiencies.

There is not an equal distribution of wave's planet wide. There are many areas where wave amplitudes are consistently large, typically closer to the poles. The challenge is finding a location to place the buoy where the waves are consistently large enough to meet the power demands of the area. The buoy must then be optimized for the amplitudes that are prevalent in that area. Correctly choosing the site will maximize the cost per kilowatt produced. Anchoring the buoy becomes another problem directly correlated to the site.

Anchoring the buoy cannot be accomplished until the overall size is established. The completed prototype that was built this year must be scaled up to a practical size where production can be accomplished on the order of 500kW. There will be many growing pains due to this increased



size. It will be necessary to construct a much stronger buoy, most likely out of steel or fiberglass. A special generator will need to be developed in order to optimize electrical power output. Many other major changes will need to be engineered in order to make scaling this buoy up to a usable size.

Unlike the buoy that could be designed for a range of amplitudes, although it is optimized for a specific one, the anchoring system is almost always unique to the site. This does not mean that a few different types cannot be designed to work in almost all practical applications. The more complex the anchoring system becomes the more expensive it will be to produce and maintain, therefore anchoring must be a consideration when choosing the site as well. Once the buoy has been scaled to a reasonable size, the necessary anchoring forces will need to be developed.

Finally and perhaps the most important aspect of future possibilities is maximizing the efficiency of the buoy. There are many aspects that need to be investigated as to maximizing the efficiencies. These include the size of the buoy; aspect ratios will play an important role in maximizing the energy that can be extracted from the wave front. Shape of the buoy is also very important for minimizing the tipping moment that could be placed on the buoy as the wave front comes in contact with the initial edges of the buoy. Maximizing efficiency in the power conversion process will also be very important. This will likely include investigating different forms of power conversion in great detail as well as designing a generator that will work most efficiently with the design.



In addition to the  $V_{oc}$  and power vs. RPM, a better motor and/or power supply is needed to test the short-circuit current ( $I_{sc}$ ) vs. RPM to compare to the manufacturer's. The reason for obtaining the  $V_{oc}$  and  $I_{sc}$  vs. RPM is to calculate the resistive load on the generator which will provide the maximum power out dependent on the angular velocity of the generator. The resistive load that provides maximum power is equivalent to the Thevenin resistance ( $R_{Th}$ ) where  $R_{Th} = \frac{V_{oc}}{I_{sc}}$ .

Maximizing efficiency will provide the grounds for future senior projects. Much of the future direction of this project requires large capital backing that will not be obtainable during a student project. However, it is the hope of this senior project team that the department begins backing this research and in the future a spinoff company can be created and that devotes itself to the advancement of this project. Hopefully the work done this year will provide a useful platform for a senior project next year as well as provide a platform for generating excitement in this field at the University of New Hampshire.



## REFERENCES

Berteaux, H. O. Buoy Engineering. New York: John Wiley & Sons, Inc., 1976.

Dean, Robert G., and Robert A. Dalrymple. Water Wave Mechanics. Englewood Cliffs: Prentice-Hall, Inc., 1984.

Falnes, Johannes. Ocean Waves and Oscillating Systems. Cambridge: Cambridge UP, 2002.

"Instantaneous Wind Energy Penetration in Isolated Electricity Grids: Concepts and Review." ScienceDirect. 25 Apr. 2008 <[www.sciencedirect.com/science?\\_ob=ArticleURL&\\_udi=B6V4S-4F29HP9-2&\\_user=1967573&\\_rdoc=1&\\_fmt=&\\_orig=search&\\_sort=d&view=c&\\_acct=C000053403&\\_version=1&\\_urlVersion=0&\\_userid=1967573&md5=0fe6bac5e46f332fb731a19753b97f70#SECX11](http://www.sciencedirect.com/science?_ob=ArticleURL&_udi=B6V4S-4F29HP9-2&_user=1967573&_rdoc=1&_fmt=&_orig=search&_sort=d&view=c&_acct=C000053403&_version=1&_urlVersion=0&_userid=1967573&md5=0fe6bac5e46f332fb731a19753b97f70#SECX11)>.

"Ocean Energy." Energy Kid's Page. DOE. 25 Apr. 2008  
<<http://www.eia.doe.gov/kids/energyfacts/sources/renewable/solar.html>>.

"Wave Dragon ... for a Better Future." 25 Apr. 2008  
<[www.wavedragon.net/index.php?option=com\\_content&task=view&id=39&Itemid=65](http://www.wavedragon.net/index.php?option=com_content&task=view&id=39&Itemid=65)>.



## APPENDIX

A.1 ALTERNATIVE BUOY SYSTEMS CONSIDERED IN DESIGN PROCESS .....	A2
A.2 SPAR DISPLACEMENT .....	A5
A.3 OPTICAL POSITIONING INSTRUMENTATION AND EVALUATION (OPIE) .....	A5
A.4 GENERATOR TESTING .....	A6
A.5 SIMULATOR DESIGN .....	A8
A.6 SIMULINK MODEL.....	A10
A.7 BILL OF MATERIALS.....	A11



### ***A.1 Alternative Buoy Systems Considered in Design Process***

One type of energy converter is the reservoir buoy. This buoy takes advantage of water flowing through a turbine. As seen in Figure 21, waves crash into a floating wall structure and the water flows over the wall into the reservoir. The water passes through a turbine at the bottom of the reservoir as it flows back into the ocean. The turbine creates power by using a generator that converts the mechanical energy to electrical energy. An advantage of this system is that it

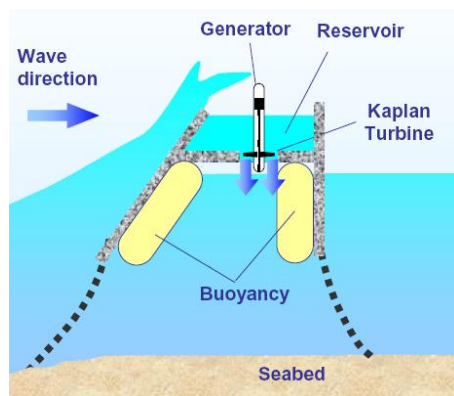


**Figure 20: Reservoir**

(<http://hydropower.id.doe.gov>)

does not have to be rigidly mounted to the base of the ocean floor. With an efficient turbine, this can be a very efficient device. The hard part is getting water in the reservoir to flow through the turbine. This is what makes the reservoir buoy less efficient. If the waves are not big enough to break over the wall, the buoy will not produce power.

Other disadvantages of the reservoir buoy are its size and environmental impact. A current model of the reservoir type buoy is called the Wave Dragon. The Wave Dragon is 57m wide and weighs 237 tons. After three years of testing, the Wave Dragon proved to be 18% efficient when comparing the total energy in the waves to the electrical energy captured<sup>1</sup>.



Another type of energy converter is an electromagnetic device, as shown in Figure 22. This is a buoy that takes advantage of the vertical motion of the waves. It is similar to a flashlight that must be shaken to provide light. This buoy has a magnetic shaft that is rigidly mounted to the ocean floor by a static member. In addition, an electric coil surrounds the magnetic

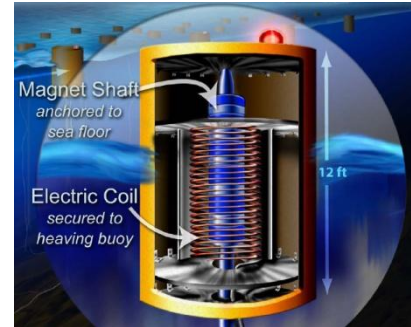


**Figure 22: Electro Magnetic**  
(<http://hydropower.id.doe.gov>)

shaft. As the buoy moves up and down with the waves, it creates electricity between the electric coils and the magnetic shaft. The disadvantage of this system is that the vertical motion of the wave is slow and does not provide much power output. Also, the buoy must be rigidly mounted to the ocean floor. This means it cannot be too far offshore or it would be too difficult to securely mount it to the bottom. A rigidly mounted system also has to withstand current drag.

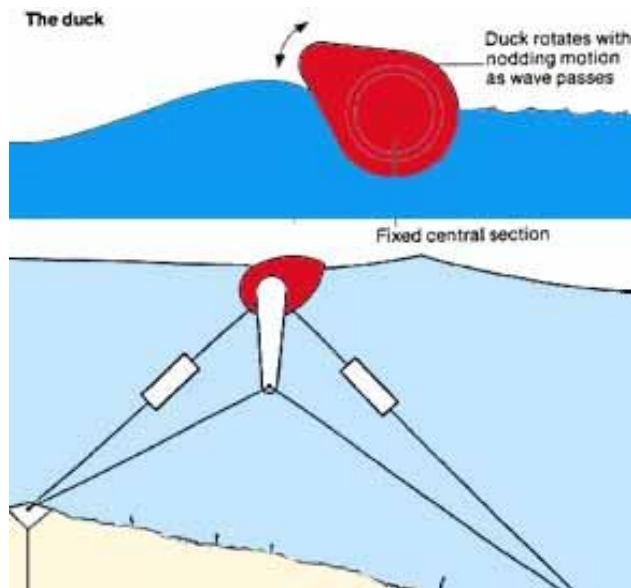


**Figure 23: Oscillating** (<http://www.fujitaresearch.com>)

Figure 23 shows another system used to capture wave energy. This system operates as an inverted pendulum. The buoy is free to oscillate with the ocean waves and it is not constrained to the vertical motion of the wave like the electromagnetic system. However, the required mooring system is complicated and must be rigidly mounted in more than one place. Additionally, the system





has moving parts under the water in the ocean. This makes it difficult to prevent both corrosion and clogging from ocean debris. This type of device uses a turbine to create electrical energy. This is done by using a tube of air and water that move back and forth through the turbine. The turbine spins a generator that provides electrical energy. A bi-directional turbine would be most effective in this device.

The final type of energy converter researched was a linear/rotating mechanical buoy seen in Figure 24. As with the electromagnetic system, this is constrained to the vertical motion of the wave. The buoy moves up and down with the wave and that motion is converted to electrical energy by any type of power conversion. The type of power conversion used defines whether it is a linear mechanical buoy or a rotating mechanical buoy. There are many power

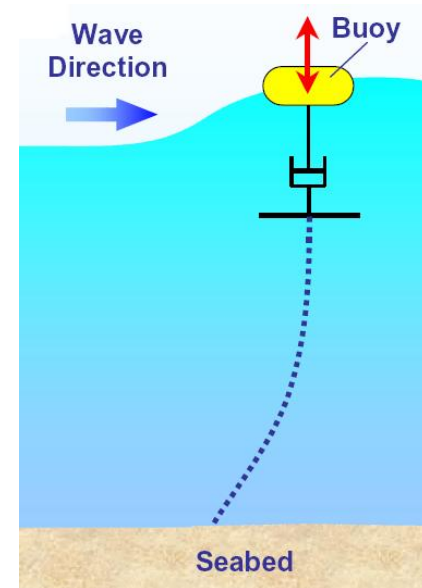


Figure 24: Linear/Rotating Mechanical buoy (<http://hydropower.id.doe.gov>)

conversion options for this type of buoy that will be described in the next section. This system has two options for mooring. It can either be rigidly supported from the ocean floor or have a slack anchoring line. If it is rigidly supported the buoy will get much more vertical motion out of the wave than if it is held with a slack line. As stated before, it is difficult to moor rigidly to the ocean floor and it constrains the location of the buoy in the ocean. For this reason, using a slack mooring line is preferable.

## A.2 Spar Displacement

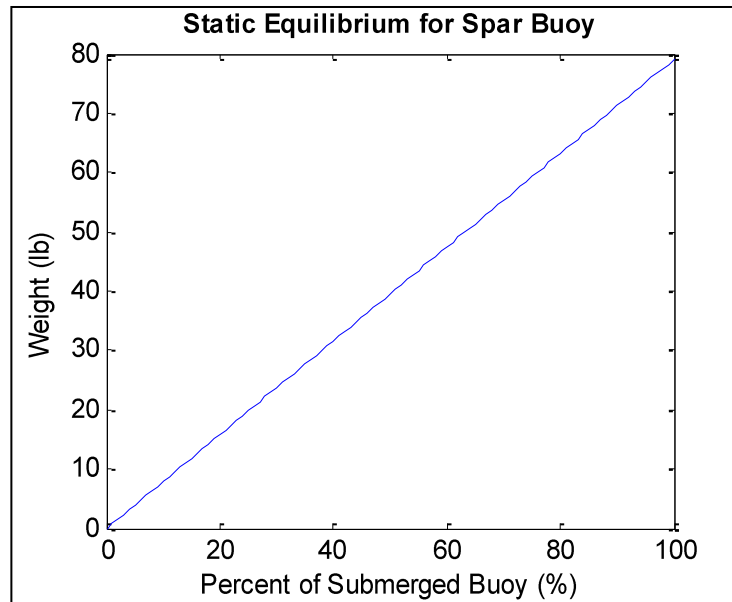


Figure 25: Static Equilibrium of Spar Buoy

## A.3 Optical Positioning Instrumentation and Evaluation (OPIE)

The software for OPIE tracks small black dots located on the spar and follower buoys. The

black dots are a

specific size, and the

size is recorded in

the OPIE software.

This is extremely

crucial because the

accuracy and size of

the dots determines

the tolerance in the



Figure 26: Calibration Dot



accuracy of the results. This is because within each frame, the software tracks a pixel within the dot. If the dot is large, the next frame could select any pixel within the dot to track. This means that the recorded amount of displacement can be significantly larger or smaller than the actual displacement. The pixel displacement on the screen is then converted to traditional units of displacement. A black calibration dot on the end of a stick must be held next to the buoy system at the start of the test, as seen in Figure 26. This is so that the software knew how many pixels in the view corresponded to a dot that size.

#### ***A.4 Generator Testing***

The input for the motor driving the generator can either be directly powered from a power supply or from a function generator, see Figure 27 below. If the function generator is going to be used, the output from the function generator needs to be the input to a power operational amplifier (op-amp), whose output then becomes the input for the drive motor. The power op-amp is needed because the function generator is unable to provide enough power.

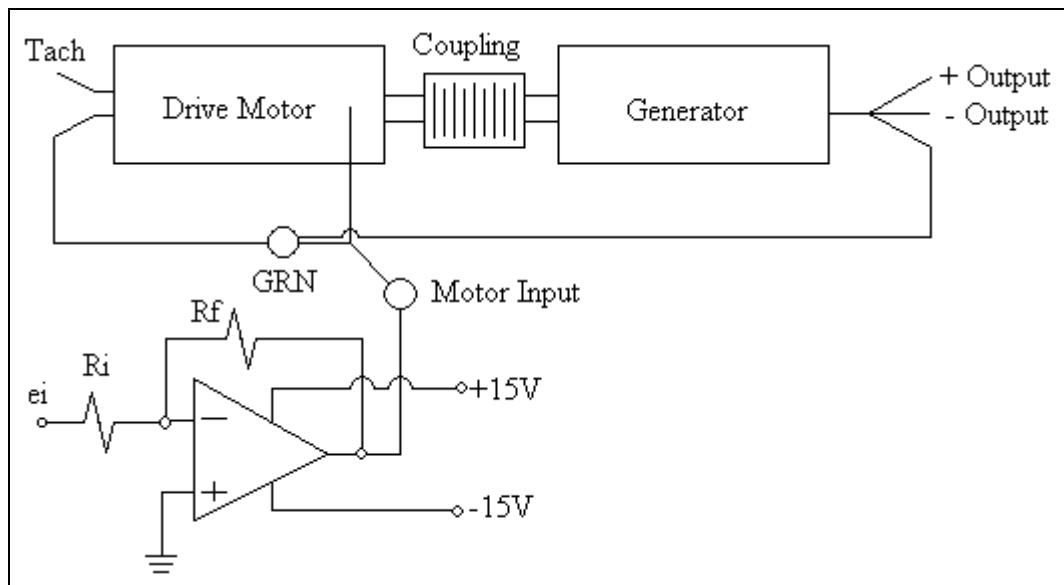


**Figure 27: Experimental Setup**

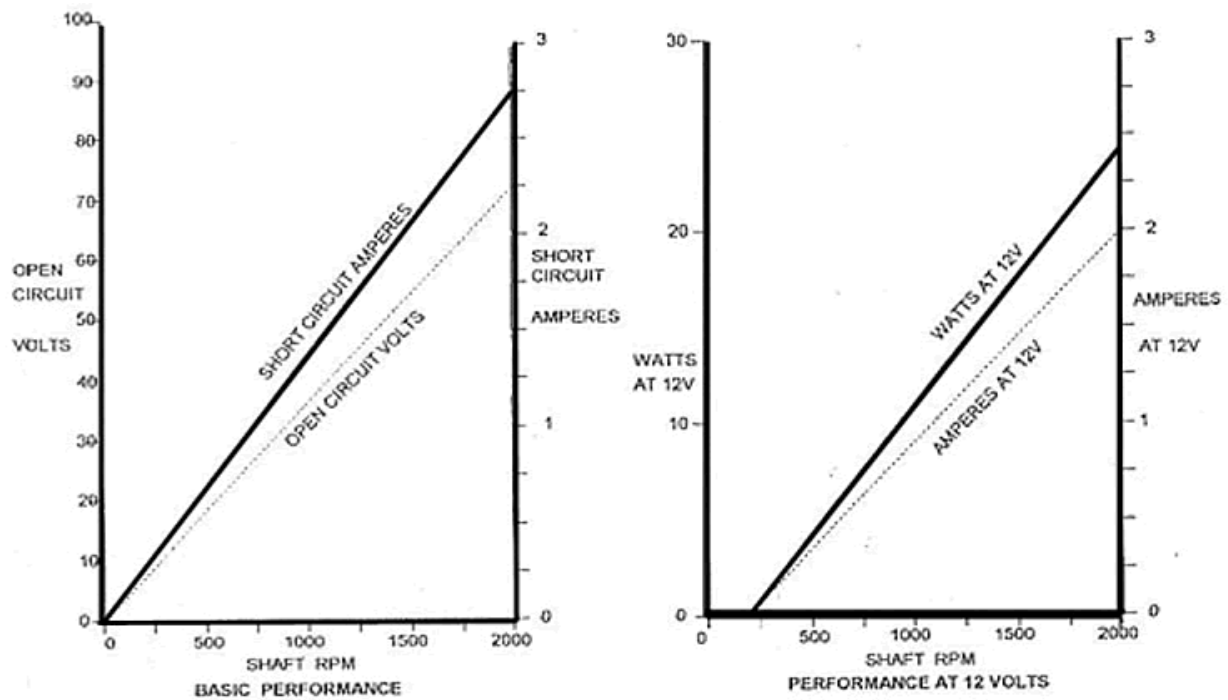


Figure 28: Windstream Power PMDC Generator Output Curves

A square input wave was used to find the time constant of the generator. It had an amplitude of  $\pm 3V$  and a three second period, as seen Figure 29 and Figure 30 below.

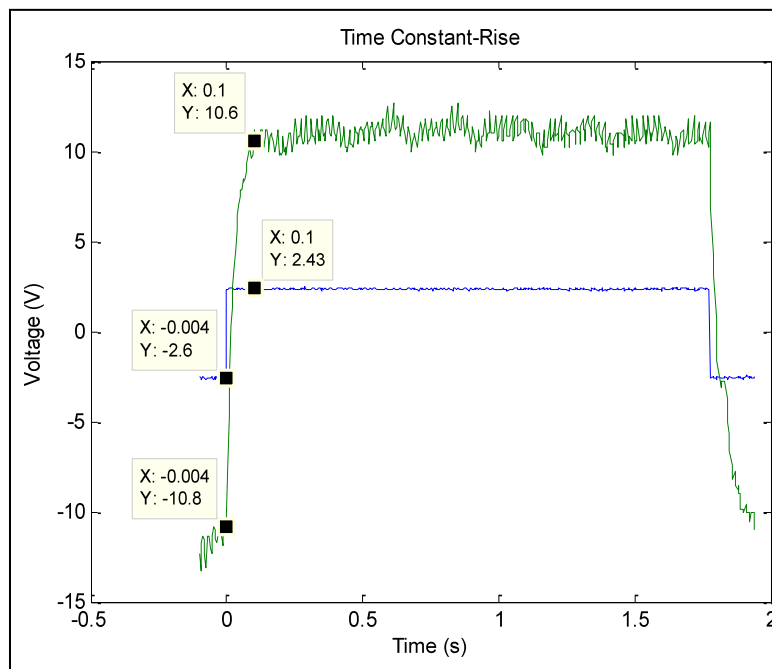


Figure 29: Time Constant of Rise with a Square Wave Input

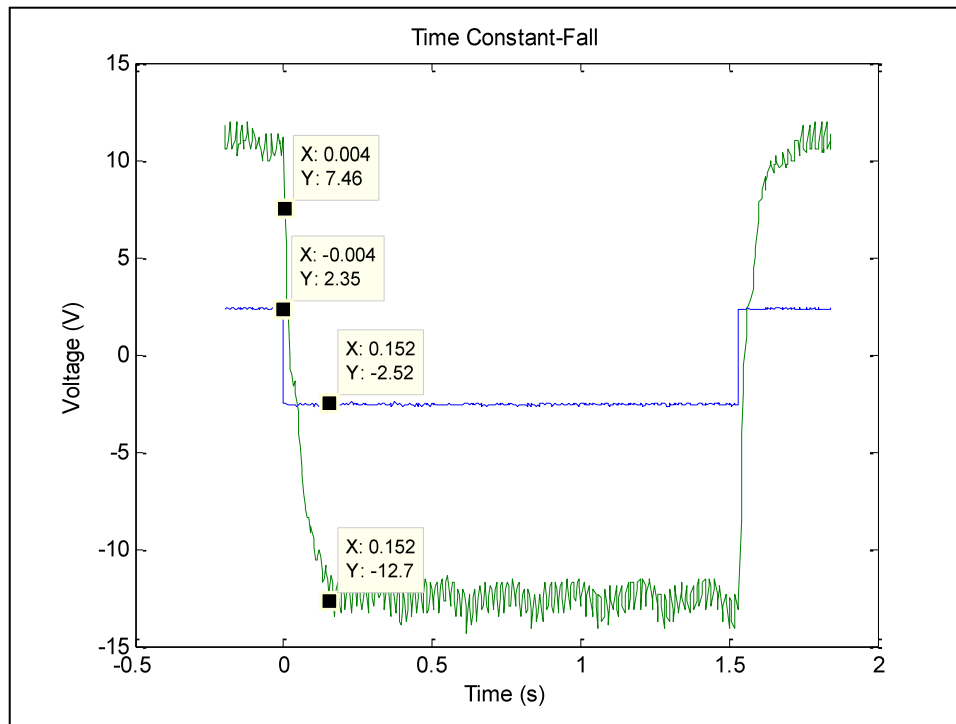


Figure 30: Time Constant of fall with a Square Input Wave

### A.5 Simulator Design

The first step in building the test simulator was designing a way of raising and lowering the spar buoy. The original design included a cam that would rotate underneath the spar, as seen in Figure 31. This would raise and lower the spar in the desired manner. However, this design was not used because of the complexity in cam geometry. Designing the shape of the cam would be extremely difficult and the geometry of the lower portion of the spar would have to be modified as well.

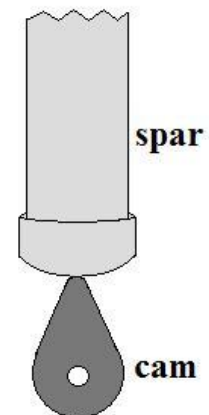


Figure 31: Cam Design

The design selected for the test simulator utilized a crankshaft. A close up image of the crankshaft can be seen in Figure 32 and the Pro Engineer model in Figure 33.



**Figure 32: Crankshaft**

The crankshaft consists of two aluminum arms and two steel pins. The aluminum arms pivot about the pins using nylon sleeve bearings. The arms are held onto the pins using e-style snap rings. The smaller crank arm is exactly half of the desired amplitude. This is because the motion of the spar is twice the length of the small crank arm. The smaller arm is held onto the shaft of the motor using a transtorque bushing. As seen in the figure, a wooden guide

was designed to keep the motion of the spar as vertical as possible.

The most crucial aspect of the test simulator is the motor. The motor was selected based on initial hand calculations of the torque necessary to raise and lower the spar buoy. The maximum load torque on the motor can be seen below.

$$T = mgr$$

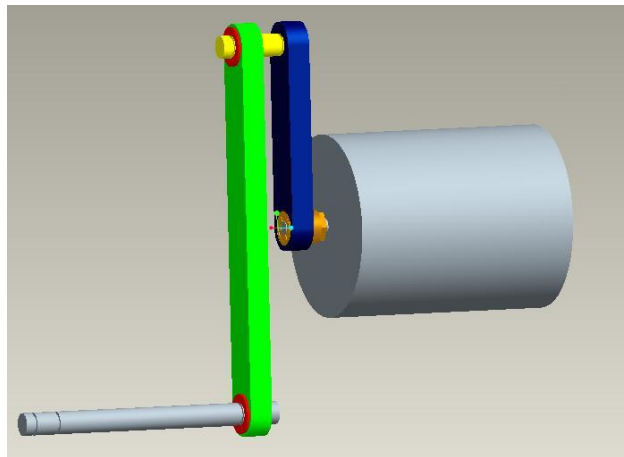


**Figure 33: ProE Model of Simulator**

In this equation, T is the load torque on the motor, m is the mass of the spar buoy, g is gravity, and r is the length of the small crank arm. The max load torque was calculated to be roughly 62.5in-lb. There was also kinematic analysis done on the slider crank system. This type of



analysis is more accurate and uses the geometries of the whole slider crank system to find the actual torque on the motor at all times. Through the kinematic analysis the max torque was found to be 82.4in-lb. A DC gear motor (brush) was selected because of its high torque values at low RPMs. The motor is rated for 180in-lb of torque at 30RPM's.

### ***A.6 Simulink Model***

The Simulink model was developed using heave wave theory which is based on the following equations. The equations are derived from vibration analysis of a system (the buoy) with a base excitation (wave motion). The following equations were used to derive the final equation listed below.

$$y = r\cos(\omega t)$$

$$\dot{y} = -\omega r\sin(\omega t)$$

$$\ddot{y} = -\omega^2 r\cos(\omega t)$$

$$\rho g A x + b \dot{x} + m_v \ddot{x} = (\rho g A y + b \dot{y} + m' \ddot{y}) e^{-kD}$$

The left side of the equation represents the motion of the buoy where its displacement is represented by the variable,  $x$ . The right side of the equation is the forced input to the buoy system. Since this is a base excitation problem based on the motion of the wave, the base input displacement is represented by variable  $y$ . The coefficients are derived from the weight of the water displaced where  $\rho$  is the density of the displaced fluid,  $g$  is gravitational acceleration, and  $A$  is the cross sectional area. The other coefficients are the damping of the fluid as well as two mass coefficients. The mass coefficients are the virtual mass,  $m_v$ , and the added mass,  $m'$ .



These mass factors include the mass of the object as well as the mass of the fluid that clings to that object.

**Table 4: Max Relative Displacement Peak to Peak**

<b>Maximum Relative Displacement Peak to Peak</b>									
	<b>Theoretical</b>	<b>Experimental</b>							
<b>Anchor Configuration</b>	(cm)	Test 1 (cm)	Difference	Test 2 (cm)	Difference	Test 3 (cm)	Difference	Test 4 (cm)	Difference
<i>10 cm Loose</i>	7.309	2.157	70.49%	3.175	56.56%	5.167	29.31%	6.716	8.11%
<i>10 cm Tight</i>	9.886	11.559	16.92%	12.493	26.37%	12.10	22.46%	N/A	N/A
<i>20 cm Loose</i>	14.639	5.909	59.64%	11.197	23.51%	10.36	29.23%	9.563	34.67%
<i>20 cm Tight</i>	19.803	22.085	11.52%	20.739	4.73%	21.09	6.49%	N/A	N/A

## **A.7 Bill of Materials**

**Table 5: BOM for Buoy**

<b>BUOY - BOM</b>				
<b>Part</b>	<b>Description</b>	<b>P/N</b>	<b>Quantity</b>	<b>Price</b>
Pinion	14.5deg	6325K88	1	16.27
Rack	14.5deg	6295K12	1	21.25
Gear 1	14.5deg	6325K86	1	27.61
Gear 2	14.5deg	6325K81	1	\$8.61
Miter Gears	20deg	7297K17	2	\$6.38
4140 Steel	1/4" thick	8975K219	1	\$14.62
Steel Rod	1/2"	5227T26	1	\$18.05
Steel Rod	5/16"	5227T24	1	\$11.84
6061 Aluminum	1/2" thick	8975K219	1	\$62.61
6061 Aluminum	1/8" x 24" x 48"	89015K68	1	134.92
Square Tube	1.25"x1.25"x3'	88875K583	1	\$15.97
Square Tube	1"x1"x6'	88875K33	1	\$22.61
Bolt	1/4" x 6"	92198A566	1	\$10.88





Nut	1/4"-20	91847A029	1	\$6.20
Knob	3/8" - 16	61125K58	1	\$3.02
Washer	1/4"	98017A660	1	\$4.00
Thrust Bearing	1/2" Shaft	23915T11	2	\$53.04
Thrust Bearing Ring	1/2" Shaft	23915T71	2	\$21.82
Al Bar	1"x1"x12"	9008K141	1	\$12.48
Bolt	8-32 x 1"	1173425	50	\$3.13
Bolt	8-32 x 1.25"	23119	10	\$0.20
Bolt	M4 x 20	11103185	10	\$0.22
Shoulder Bolt	1/4" x 1.25"	26425	4	\$2.50
Shoulder Bolt	1/4" x 1"	26424	2	\$1.15
Nut	10-24	36028	6	\$0.04
Washer	#10	33074	6	\$0.02
PVC	6" Dia x 10' Long	472033	1	\$37.80
PVC Cap	6" Dia	N/A	2	\$12.41
Bolt	8-32 x 3/4"	1123116	40	\$0.66
Bolt	3/8" -16 x 3/4"	1124284	4	\$0.25
Shoulder Bolt	1/4" x 1"	1126306	7	\$1.15
Bolt	8-32 X 1/4"	73420	40	\$0.73
Standard Hex Set		0229993	1	\$3.64
Metric Hex Set		82857	1	\$6.92
Bolt	1/4-20 x 5"	92198A566	1	\$10.88
Nut	1/4 - 20	91847A029	1	\$6.20
Washer	1/4	98017A660	1	\$5.28
Drill Bit (For Foam)	1/4" x 6"	2894A62	1	\$2.54
Knob Handle	3/8-16	61125K58	1	\$3.02
Bearings	0.25"	1ZEG8	2	\$5.25
Bearings	0.3125"	1ZEH2	2	\$4.38
Linear	.05"	5KD53	1	\$52.02
Steel Rod	3/8"	2HJF5	1	\$1.59
Permanent Magnet DC Generator		N/A	1	\$159.00
Fender Washer	Box of 25		1	\$3.49
Assorted Bolts			1	\$8.38
Sealant			1	\$5.97
Caulking			1	\$1.97
Foam		N/A	1	\$50.00
				<b>Subtotal</b> \$862.97
				<b>Shipping</b> 196.07
				<b>Total</b> <b>\$1,059.04</b>

**Table 6: BOM for Simulator**

<b>SIMULATOR - BOM</b>			
<b>Item:</b>	<b>P/N:</b>	<b>Amount:</b>	<b>Cost/item:</b>
Trantorque	5926k13	1	\$33.89
Rod End	6251K16	1	\$18.26
Aluminum Plate	8975K113	1	\$15.85
Bearings	6294K223	2	\$3.00
Snap Rings	98408A138	1	\$5.56
C-Clamp		2	\$29.94
Hose Clamp		2	\$2.90
Assorted Hardware		N/A	\$1.09
2" X 4"		7	\$13.44
Plywood		1	\$10.98
Motor	GM14604S002	1	\$362.04
		<b>Subtotal</b>	<b>\$496.95</b>
		<b>Shipping</b>	<b>\$12.12</b>
		<b>Total</b>	<b>\$509.07</b>